Chapter

Nanostructured Multilayer Composite Coatings for Cutting Tools

Sergey Grigoriev, Alexey Vereschaka, Marina Volosova, Caterina Sotova, Nikolay Sitnikov, Filipp Milovich and Nikolay Andreev

Abstract

The chapter deals with the specific features concerning the application of wear-resistant coatings to improve the performance properties of ceramic cutting tools. The paper discusses the theoretical background associated with the specific operation conditions and wear of ceramic cutting tools and influencing the choice of the compositions and structures of wear-resistant coatings. The studies were focused on the application of the Ti-(Ti,Al)N-(Zr,Nb,Ti,Al)N multilayer composite coating with a nanostructured wear-resistant layer, as well as the (Cr,Al,Si)N–(DLC–Si)–DLC–(DLC–Si) and (Cr,Al,Si)N–DLC composite coatings in order to improve the cutting properties of ceramic tools. The chapter presents the results of the comparative cutting tests for the tools with the coatings under study, uncoated tools, and tools with the Ti-(Ti,Al)N commercial coating. The wear mechanisms typical for ceramic cutting tools with coatings of various compositions have been investigated.

Keywords: nanocomposite functional coating, diamond-like carbon (DLC), ceramic cutting tool, tool wear

1. Introduction

Ceramic cutting tools are more and more widely used due to their high hardness, wear resistance, and relatively low cost [1–6]. The main specific feature of cutting ceramics is the absence of a binder phase, which significantly reduces the degree of softening in ceramic cutting tools during heating and increases their plastic strength. Due to the above, the cutting process can imply high cutting speeds, which significantly exceeds the cutting speeds typical for the machining with carbide cutting tools [1, 2, 5, 6]. While for a carbide cutting tool, the limiting level of cutting speeds is 500,600 m/min, then for a tool equipped with cutting ceramics, this level increases up to 9,001,000 m/min and higher [1]. However, the absence of the binder phase also has negative influence on the performance properties of ceramic cutting tools. In particular, their brittle strength, impact toughness, and resistance to crack formation decrease [1–4]. This fact significantly influences the wear patterns on ceramic cutting tools. For example, low crack resistance provokes the formation of a crack front, which, due to the absence of a plastic binder phase,

encounters no barriers to slow down or stop the crack development. The above is the main reason for micro- and macrochipping on contact pads of a ceramic cutting tool already at the stages of running-in or initial steady-state wear, causing failures because of brittle fracture. The noted wear mechanism prevails on ceramic cutting tools, and it actually does not depend on the cutting speed, because the temperature factor does not have a noticeable influence on the transformation of the wear mechanism. To a large extent, it is this mechanism of wear which determines the scope of application of the ceramic cutting tools [6–12].

At present, ceramic cutting tools are usually recommended for the finishing of gray, malleable, high-strength, and chilled cast irons, low- and high-alloy steels, including improved and heat-treated (up to HRC 55–60) non-ferrous alloys and structural polymer materials (K01 K05, P01 P05) [1–6]. Under the above conditions, tools equipped with ceramic cutting inserts are noticeably superior to carbide cutting tools in terms of working efficiency.

During the intermittent cutting, the use of ceramic tools in machining with advanced values of cross-section of cut ($a_p \times f$) sharply reduces their efficiency due to the high probability of sudden failure because of the brittle fracture of the cutting parts of the tools [1, 2]. This fact largely explains the relatively low volume of ceramic tools used in production sector [1, 2].

In this regard, the main direction of improving the performance activities of cutting ceramics is an enhancement of its strength characteristics to expand the area of the technological application in cutting. Recently, a new class of tool materials has appeared attributed to the group of cutting ceramics with increased strength, toughness, and crack resistance (silicon nitride, reinforced ceramics), and this fact indicates that the scope of application of ceramic cutting tools expands noticeably [1–6].

2. Theoretical background

The operation conditions for ceramic cutting tools significantly differ from those under which tools of high-speed steel and carbides are used. A substantial increase in cutting speed changes the mechanism of chip formation and contact processes during the cutting, as well as the nature and level of power and temperature loads, thermomechanical stress, and mechanisms of tool wear [13–15]. The results of the studies focused on the stress state in the cutting part of a ceramic tool [16] indicate the presence of tensile and compressive stresses (**Figure 1**). At the

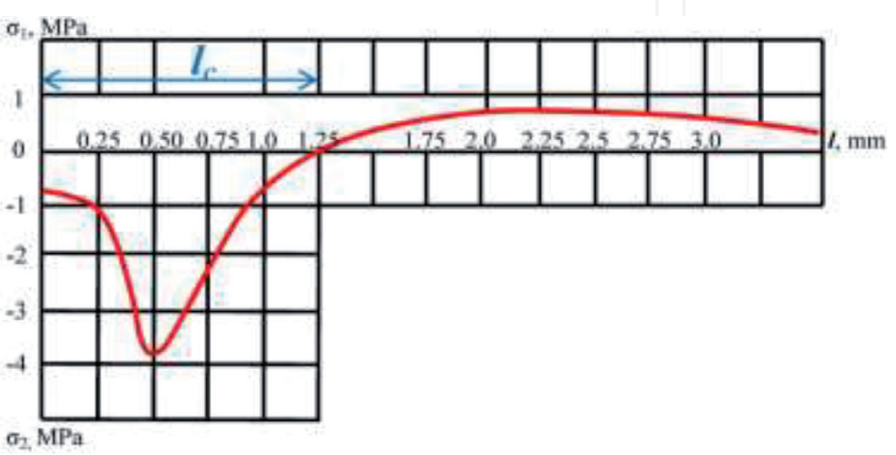

Figure 1.
Distribution of principal stresses σ_1 and σ_2 along the rake face of a cutting tool [1, 2].

same time, in most cases, the area of tensile stresses begins at the end of the contact area of the chips with the rake face. When section thickness is small, compressive stresses prevail, while at larger thicknesses, tensile stresses begin to play a significant role [17, 18].

The most stressed section in the tensile area is located on the rake face of the tool at a distance equal to (2–2.5)*lc*, where *lc* is the length of contact between the chips and the rake face of the tool.

With a decrease in the rake angle γ, the compression area extends, and the tensile area decreases or disappears at all. As a result, the negative angle γ is typical for a ceramic cutting tool and makes it possible to achieve a change in the stress state in the direction of the predominantly compressive stresses [17, 18]. Deposition of a coating on a cutting tool significantly changes the nature of the interaction between the material being machined and the tool. In [19, 20], the studies revealed that the coating parameters had a significant influence on the characteristics of the contact processes and the chip formation. To prevent a sudden failure of a ceramic cutting tool as a result of brittle fracture, it is necessary to control the processes of the contact interaction between the tool material and the material being machined by depositing coatings on the working surfaces of the tool. The composition and structure of such coatings will increase the length of the full contact between the chips and the rake face of the tool through enhancement of the adhesion to the material being machined and the improvement of heat removal from the cutting area due to increased thermal conductivity of the tool material. Thus, the specific thermomechanical loads on the cutting edge of the ceramic tool can be reduced (see **Figure 2**).

There are a number of studies considering the use of coatings to improve the performance properties of ceramic cutting tools, with both oxide and nitride ceramics as the ground. In [21], the investigation is focused on PVD of the (Ti,Zr)N-(TiN/ZrN) and TiN-(TiAl)N-(TiN/(TiAl)N) nanostructured multilayer coatings, deposited on ceramic cutting inserts of Al_2O_3 + ZrO_2 + Ti(C,N) and Al_2O_3 + TiC, with the external layer formed by the alternating nanolayers of TiN and ZrN or TiN and (Ti,Al)N, respectively. With the total coating thickness of 3–5 μm and the microhardness of about HV 29 GPa, the above coatings prolonged the tool life by 20–80% during the dry cutting of NC6 steel (HRC 48–52), at v_c = 150 m/min, f = 0.10 mm/rev, a_p = 0.5 mm.

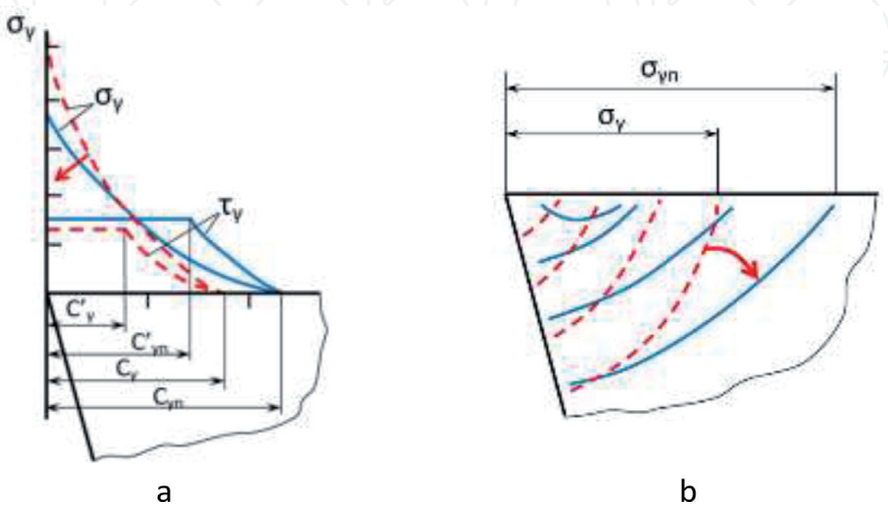

Figure 2.
Differences in (a) stresses and (b) isotherms for a coated and uncoated tool: C_γ and $C_{\gamma m}$ - the total lengths of the contact between the chips and the rake face of the uncoated (the dashed line) and coated (solid line) tools, respectively; changes in stresses and isotherms occur in the direction of the arrows [1, 2].

In [22], the studies considered the properties of a ceramic cutting tool with the PVD coating of TiN-(Ti,Al,Si)N-TiN with the thickness of 2–4 μm with a nanostructured layer of (Ti,Al,Si)N and the CVD coating of TiN-Al_2O_3 with the thickness of 2.6–10 μm, when inserts of nitride ceramics of Si_3N_4 and oxide ceramics of Al_2O_3 + ZrO_2 were used as substrates. The cutting properties were used during the turning of EN-GJL-250 gray cast iron and C45E steel. The cutting process was carried out under the following conditions: f = 0.10, 0.15, and 0.20 mm/rev; a_p = 1 and 2 mm; v_c = 200 and 400 m/min. The cutting tools with coatings of all types demonstrated the longer tool life compared to that of the uncoated tools, while the longest tool life was detected for the tools with the PVD coating of TiN-(Ti,Al,Si)N-TiN with the nanostructured middle layer. In [23], the studies considered the cutting properties of tools made of mixed ceramics of Al_2O_3 + TiCN with the TiN commercial coating during the turning of hardened American Iron and Steel Institute (AISI) 52,100 (HRC 63) steel under the following cutting conditions: f = 0.07, 0.11, and 0.14 mm/rev, a_p = 0.5 mm, v_c = 100, 150, 200, 250, and 300 m/min. The studies found that for the uncoated cutting inserts, wear in the form of cracking and chipping was more typical, while for the coated tools, the formation of a wear crater on the rake face was typical. The cutting path for the coated tool was about 8 times longer, and the temperature in the cutting area was substantially lower than for the uncoated tool.

According to the results of [24], which studied the cutting properties of tools made of silicon nitride (Si_3N_4) with the CVD coating of TiN-Al_2O_3 during the continuous turning of gray cast iron with various depths of cut, the prevailing failure mechanism for the above cutting tools was abrasive wear during the continuous turning and a combination of abrasive wear and brittle fracture during the machining with variable depths of cut. The coated cutting tools demonstrated much longer tool life compared to the uncoated cutting tools: the length and time of cutting were about 3.5 times longer at the cutting speed of 300 m/min and 2 longer at the cutting speed of 380 m/min.

The cutting properties of ceramic tools of Si_3N_4 with the PVD coating of (Ti,Al)N-(Al,Cr)O during the turning of HT250 gray cast iron and AISI 4340 steel were studied in [25]. The thicknesses of the (Ti,Al)N and (Al,Cr)O layers were about 2.0 and 0.6 μm, respectively. The tool life of a tool made of silicon nitride with the (Ti,Al)N-(Al,Cr)O coating was longer compared to uncoated inserts during the turning of gray cast iron and steel. In [26], authors investigated the cutting properties of tools based on silicon nitride with the PVD coatings of $(Ti_{0.5},Al_{0.5})N$ and $(Cr_{0.3},Al_{0.7})N$ during the dry turning of gray cast iron. For the tools with the $(Ti_{0.5},Al_{0.5})N$ and $(Cr_{0.3},Al_{0.7})N$ coatings, the tool life was at least 2 times longer compared to the uncoated tools. The tools with the $(Ti_{0.5},Al_{0.5})N$ coating demonstrated longer tool life compared to the tools with the $(Cr_{0.3},Al_{0.7})N$ coating. In [27], the studies are focused on the cutting properties of tools made of the Al_2O_3 + TiC mixed ceramics with the TiN-(Al,Cr)N multilayer coating during the dry turning of AISI 4340 (HRC 46) hardened steel at v_c = 125–175 m/min, a_p = 0.25–0.63 mm, f = 0.10–0.25 mm/rev. After 9 minutes of cutting, the wear VB was on average 45% higher for the uncoated tool.

The application of diamond-like carbon (DLC) coatings for ceramic cutting tools should be considered separately. While several studies consider the properties of DLC, deposited on a ceramic substrate, there are hardly any investigations focused on ceramic cutting tools with DLC coatings. For example, in [28, 29], the studies consider the challenges of improving the performance properties of ceramic tribological pairs (sliding bearings). A significant decrease in the coefficient of friction (COF) was noted with the use of samples with DLC coatings. Ceramic products

made of SiC with DLC coatings demonstrate excellent chemical stability, low COF, and very good wear resistance [30]. The properties of DLC coatings deposited on the Si_3N_4 substrate were also considered. Gomes et al. [31] studied the tribological properties of uncoated samples and samples with the DLC and DLC-Si coatings under friction, paired with counterbodies made of stainless steel. Both coatings demonstrated good tribological properties, but samples with the DLC-Si coating separated from the substrate, and the wear coefficient for samples with the DLC coating was much lower compared to samples with the DLC-Si coating. As a result of the studies considering the properties of mechanical face seals of nitride ceramics with the DLC and DLC-Si coatings, it was found that the use of these coatings significantly reduced the COF and improved wear resistance of products. At the same time, the DLC coatings look more preferable compared to DLC-Si coatings [32]. Following the results of the investigation focused on the properties of the DLC coating, deposited on the substrate of Si_3N_4 and M50 steel, it was found that the normal stresses on the boundary of the "coating–substrate" interface were higher (by about 10%) for the ceramic substrate, which could be explained by the higher value of the elastic modulus of Si_3N_4 [33]. It has also been found that as the coating thickness grows from 200 up to 400 nm, the stresses decrease at the boundary of the "coating–substrate" interface in accordance with the quadratic expression, and such a decrease slows down with the growth of the coating thickness [34]. A sample with the DLC coating demonstrates a lower COF compared to a sample with the MoS_2 coating [35]. Following the investigation focused on the tribological properties of a sample with the Cr-DLC coating under friction, paired with uncoated counterbodies of Al_2O_3, ZrO_2, Si_3N_4, and WC in air and in the helium atmosphere, it was found that the tribological properties of the samples with the DLC coating were significantly higher in air than in the helium atmosphere [36]. Two-dimensional finite element modeling of the properties of the DLC coating, deposited on the substrate of Al_2O_3 exhibited that a growth of the DLC coating thickness led to an increase in its hardness and crack resistance [37]. The studies revealed the ability of the DLC coating to minimize surface defects on the substrate and significantly reduce the intensity of oxidation processes [38]. The DLC coatings deposited on the substrate of β-SiAlON increase the surface hardness and improve the surface quality [39]. The comparison of the tribological properties of the Cr_2O_3-based samples with the DLC, TiN, and TiAlN coatings and of the uncoated samples in contact with cast iron counterbodies found that the samples with the DLC coatings demonstrated the highest scuffing resistance and the lowest coefficient of friction (COF) [40]. The studies carried out in air and in water environment, in nitrogen atmosphere, and in vacuum revealed a significant decrease in the COF, an increase in wear and oxidation resistance after deposition of the DLC coatings on the substrates of SiC, Si_3N_4, and ZrO_2 [41, 42]. Close values of the elastic modulus of the coating and the substrate is an important factor able to reduce internal stresses and thus improve the service life and reliability of products with the DLC coatings. At the same time, the deposition of coatings, in particular, the DLC coatings, on ceramic products increases their wear resistance, significantly reduces the COF, and enhances the oxidation resistance. Another important factor is also a leveling effect of a coating, which minimizes the influence of microconcentrators of stresses (pores, microcracks, etc.) on the reliability and service life of a product, while reducing the surface roughness value is important. Meanwhile, many studies note such a problem as the low strength of adhesive bonds between a DLC coating and a ceramic substrate, which leads to failure of the coating due to its separation from the substrate. Another important challenge is to study the influence of Si on the properties of the DLC coatings and the cutting properties of tools with such coatings.

3. Materials and methods

Multicomponent coatings of Ti-(Ti,Al)N-(Zr,Nb,Ti,Al)N with three-layer architecture, including adhesion, transition, and wear-resistant layers [43–50] were studied. The Ti-(Ti,Al)N coating widely used as a coating for metal-cutting tools was assumed as an object of comparison. The coating was chosen with the multilayer architecture, including an (Cr,Al,Si)N adhesive-smoothing layer, a DLC-Si transition layer, and a DLC wear-resistant layer, in order to secure high adhesion to the ceramic substrate and release the smoothing effect of the coating. Following some studies [51–53], it was found that the adhesion of the coating to the substrate was enhanced due to a DLC-Si layer included in the coating. Furthermore, in [51], the studies found that the DLC-Si demonstrated lower hardness and wear resistance compared to those of the DLC coating, and that fact contributed to the selection of DLC-Si as a transition layer ensuring high adhesion and a smooth transition of properties.

The adhesion layer of (Cr,Al,Si)N can demonstrate the extremely high hardness (up to 55 GPa [54]) in a combination with significant toughness [55]. High thermal stability is another important feature of the above compound [55, 56]. Therefore, there is a possibility of a transition from a ceramic substrate (with the hardness of 15 to 20 GPa) through the (Cr,Al,Si)N layer to DLC-Si layers and a DLC coating (with the hardness from 30 to 80 GPa). Furthermore, due to its greater toughness compared to the DLC coating, the (Cr,Al,Si)N layer is able to "heal" microcracks and micropores by penetrating them on the surface of a ceramic substrate. In [57–59], the studies found that due to its nanocomposite structure, the (Cr,Al,Si)N layer improved the crack resistance while retaining high hardness.

The filtered cathodic vacuum arc deposition (FCVAD) was used to deposit the coatings of Ti-(Ti,Al)N-(Zr,Nb,Ti,Al)N and Ti-(Ti,Al)N in the VIT-2 unit [43, 60–66].

The lateral rotating cathode technology (LARC; developed by PLATIT – BCI Group, Switzerland) was applied to deposit DLC coatings on a PLATIT π-311 unit.

A nitride coating was deposited using cathodes containing Cr, Al, or Al–Si (88:12 at%). Argon (Ar) ions were subjected to purification using a beam of Ar ions at an anode voltage of 800/200 V and a current of 0.5 A for 20 min. A coating of Si-DLC was deposited using a mixture of gases, including 90% acetylene (C_2H_2), 8% Ar, and 2% tetramethylsilane ($Si(CH_3)_4$). A similar mixture of gases, except for $Si(CH_3)_4$, was used to deposit a pure DLC coating.

The microstructural investigation of samples involved a scanning electron microscope (SEM; Field Electron and Ion Company) Quanta 600 FEG.

The micro- and nanostructures of the samples were analyzed with a JEM 2100 high-resolution transmission electron microscope (HR-TEM), at the accelerating voltage of 200 kV. The energy-dispersive X-ray spectroscopy (INCA Energy) was applied to study the chemical composition of the samples.

The nanoindentation technique on an Instron Wilson Hardness Group Tukon device at the load of 0.01 N was applied to find the microhardness of the coatings. A CU 500 MRD lathe (Sliven) with a ZMM CU500MRD variable speed drive was used during the turning of workpieces made of AISI 52100 (HRC 56–58) hardened steel to study the cutting properties of the coated tool and the dynamics of its wear, at f = 0.1 mm/rev, a_p = 0.5 mm, and v_c = 320 m/min (for the tool with the DLC coatings) and ASTM T31507 hardened steel (DIN 1.2419, HRC 58–60) and ASTM X153CrMoV12 (DIN 1.2379, HRC 60–61) hardened steel v_c = 80–350 m/min; f = 0.1–0.25 mm/rev; a_p = 0.5–1.0 mm for the tool with the Ti-(Ti,Al)N-(Zr,Nb,Ti,Al)N and Ti-(Ti,Al)N coatings.

4. Results and discussion

4.1 Turning of X153CrMoV12 hardened steel with tool made of Al_2O_3-TiC and Al_2O-SiCw mixed ceramics with Ti-(Ti,Al)N-(Zr,Nb,Ti,Al)N coating

The structure of the Ti-(Ti,Al)N-(Zr,Nb,Ti,Al)N coating is depicted in **Figure 3** [67]. The total thickness of the coating is about 4 μm, and the nanolayer binary period λ is about 120 nm.

The chemical compositions of the coatings under study are presented in **Table 1**.

The coatings contain a similar amount of aluminum; however, the presence of Zr and Nb in the second coating causes some decrease in hardness with an increase in ductility, which makes it possible to provide a good level of resistance to brittle fracture [44, 46].

Figure 4a and **b** exhibit the results of the studies focused on the cutting properties of a tool equipped with (1) uncoated ceramic inserts made of Al_2O_3-TiC and Al_2O_3-SiCw ceramics, (2) Ti-(Ti,Al)N coating, and (3) Ti-(Ti,Al)N-(Zr,Nb,Ti,Al)N coating [67]. During the longitudinal turning of X153CrMoV12 hardened steel, the wear rate of ceramic tools based on mixed ceramics of Al_2O_3-TiC and Al_2O_3-SiCw depends rather largely on the coating composition. In particular, the maximum increase in the wear resistance of ceramic tools was provided by coatings based on the complex composite nanostructured system of Ti-(Ti,Al)N-(Zr,Nb,Ti,Al)N. At VB = 0.4 mm, the above system increases the tool life of a ceramic tool up to 1.5 times compared to an uncoated tool and by 1.3 times compared to a tool with the Ti-(Ti,Al)N commercial coating.

According to the studies of [1–4, 14–18], for a ceramic tool, the brittle fracture of its cutting edge is the most probable mechanism of failure. This fact can be explained by the lower brittle strength of the ceramic tool material in comparison with the same parameters of the carbide tool material. Ceramic tools also tend to stochastic brittle fracture because of the higher contact stresses, in particular, normal stresses. In general, the above contact stresses exceed the same values for carbide tools because of the considerable decrease in the total length of the contact between the chips and the rake face of the ceramic tool, at a small decrease in the normal load.

There are is a balance in the nature of wear centre development on the rake and flank faces of the Al_2O_3-TiC ceramic cutting insert with the Ti-(Ti,Al)N and Ti-(Ti,Al)N-(Zr,Nb,Ti,Al)N coatings during the longitudinal turning of X153CrMoV12 hardened steel, with no visible chips and microchipping.

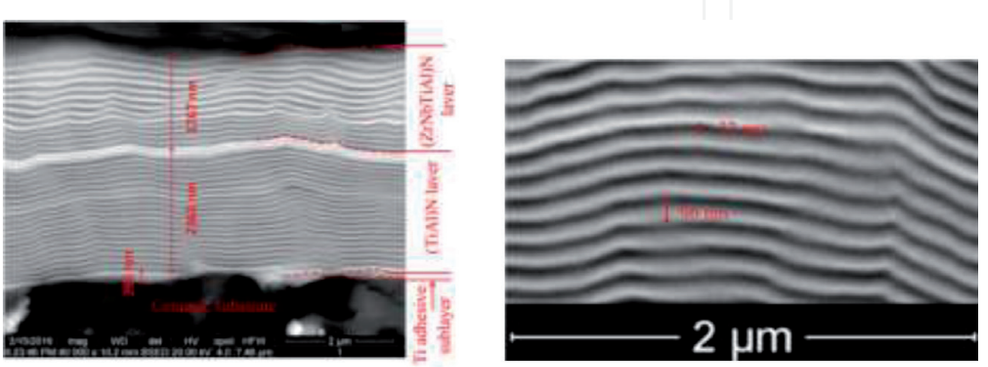

a b

Figure 3.
Micro (a) and nano (b) structure of the cross-section for cutting Al_2O_3–TiC with Ti-(Ti,Al)N-(Zr,Nb,Ti,Al)N coatings ceramic inserts [67] (SEM).

	Ti, at%	Al, at%	Zr, at%	Nb, at%
Ti-(Ti,Al)N	70	30	—	—
Ti-(Ti,Al)N-(Zr,Nb,Ti,Al)N	42	26	29	3

Table 1.
Chemical compositions of the coatings under study.

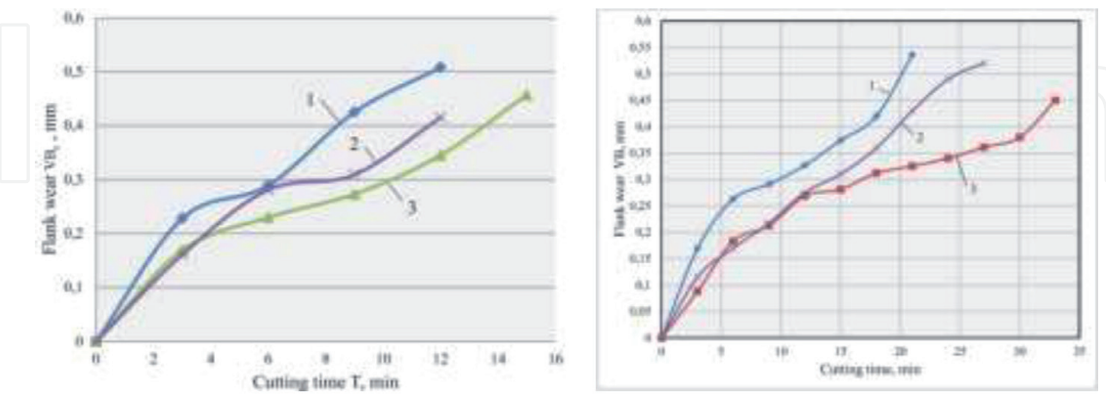

Figure 4.
Relationship between wear VBmax and cutting time for (1) uncoated inserts, (2) tools with Ti-(Ti,Al)N coating, and (3) Ti-(Ti,Al)N-(Zr,Nb,Ti,Al)N coating, during the longitudinal turning of X153CrMoV12 hardened steel at v_c = 250 m/min, f = 0.05 mm/rev, a_p = 0.5 mm, inserts made of (a) Al_2O_3-TiC and (b) Al_2O_3-SiCw at v_c = 300 m/min, f = 0.1 mm/rev, a_p = 0.5 mm, inserts made of (b) Al_2O-SiCw [67].

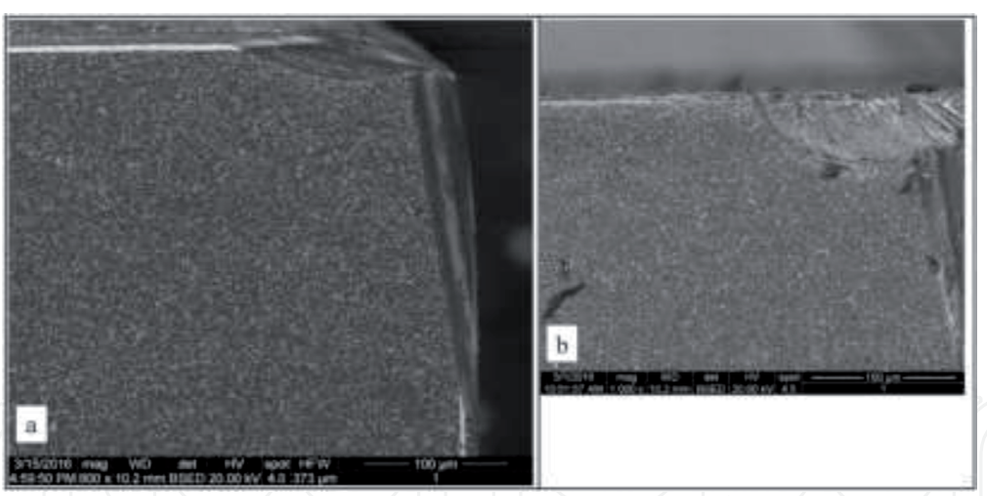

Figure 5.
Wear pattern after 25 minutes in the longitudinal turning of X153CrMoV12 hardened steel at v_c = 250 m/min, f = 0.05 mm/rev, a_p = 0.5 mm for cutting inserts made of Al_2O_3-TiC with Ti-(Ti,Al)N [67] (SEM).

Undisturbed residues of coatings at the edges of wear centres both on the rake and flank faces of the ceramic cutting insert are also typical for the process described above (**Figure 5a** and **b**) [67].

Both on the rake and flank faces of the tool, the wear mechanism typical for the Ti-(Ti,Al)N-(Zr,Nb,Ti,Al)N coating is primarily an abrasive interaction with the material being machined (**Figures 6** and 7) [67]. It should be noted that the coating and the substrate work as a unified system, where cracks and chipping hardly occur. No adherents of the material being machined are detected on the coating surface, which may relate to the low adhesion between the external (wear-resistant) layer and the material being machined.

During the cutting, good adhesion retains between the coating and the ceramic substrate (**Figure 7**) [67].

For the Ti-(Ti,Al)N-(Zr,Nb,Ti,Al)N coating, the typical mechanism of the coating failure is the formation of longitudinal cracks in the areas immediately adjacent to the cutting area (**Figure 8**) [67]. However, such cracks related to the delamination of the coating under the influence of the compressive residual stresses are much less dangerous compared to transverse cracks, often formed in monolithic coatings.

During the process of cutting with the ceramic tool with the Ti-(Ti,Al)N coating, massive adherents of the material being machined are formed, both on the rake and flank faces of the tool (**Figure 9**) [67]. The mechanism of tool wear relates to the adhesive-fatigue processes, which is confirmed by the nature of the coating failure with clear tear-outs of the coating elements (see **Figure 9**).

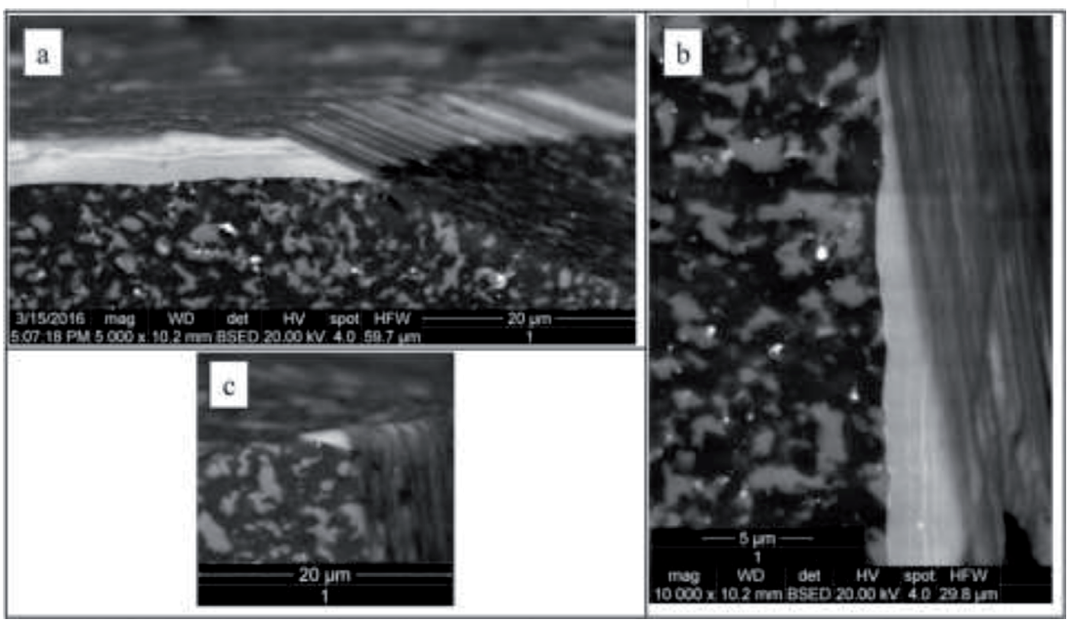

Figure 6.
Wear pattern on (a) rake face, (b) flank face, and (c) corner of the Al_2O_3-TiC ceramic insert with the Ti-(Ti,Al)N-(Zr,Nb,Ti,Al)N coating [67] (SEM).

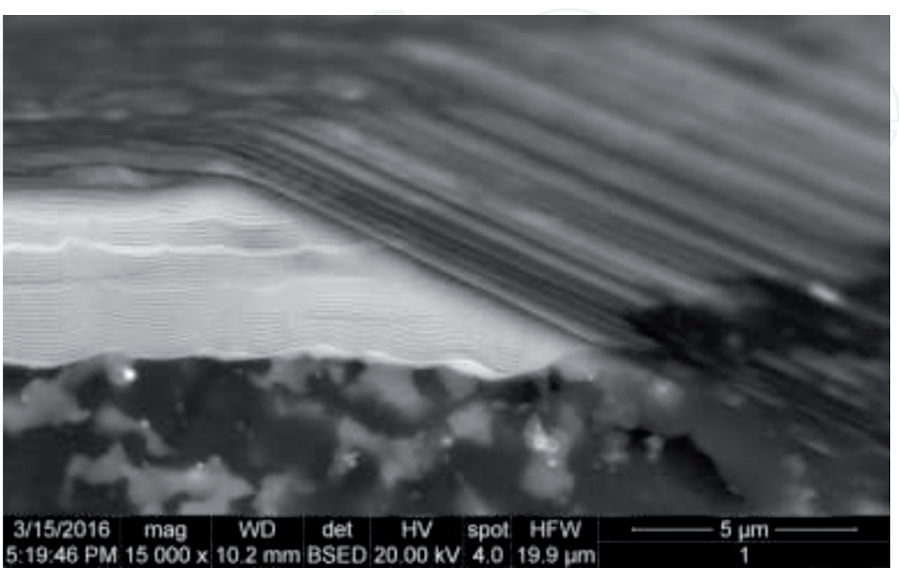

Figure 7.
Wear pattern on the rake face of the Al_2O_3-TiC ceramic insert with Ti-(Ti,Al)N-(Zr,Nb,Ti,Al)N coating [67] (SEM).

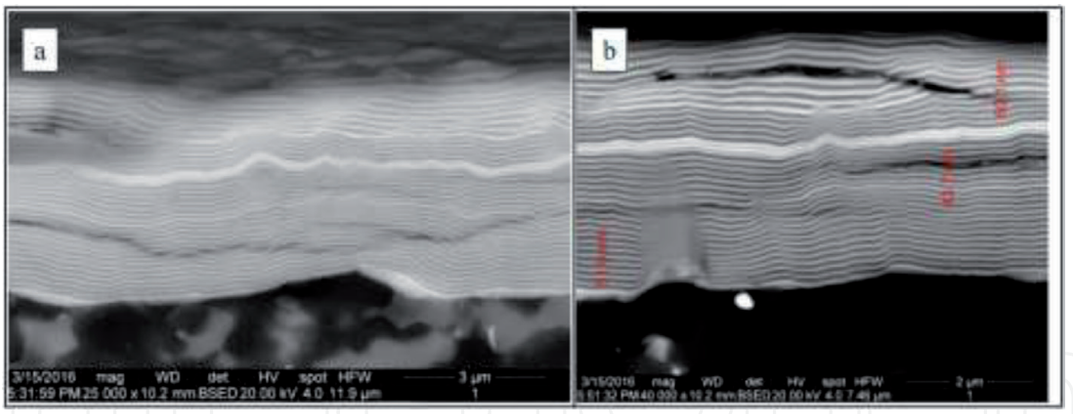

Figure 8.
Ceramic insert of Al_2O_3-TiC with the Ti-(Ti,Al)N-(Zr,Nb,Ti,Al)N coating [67] (SEM).

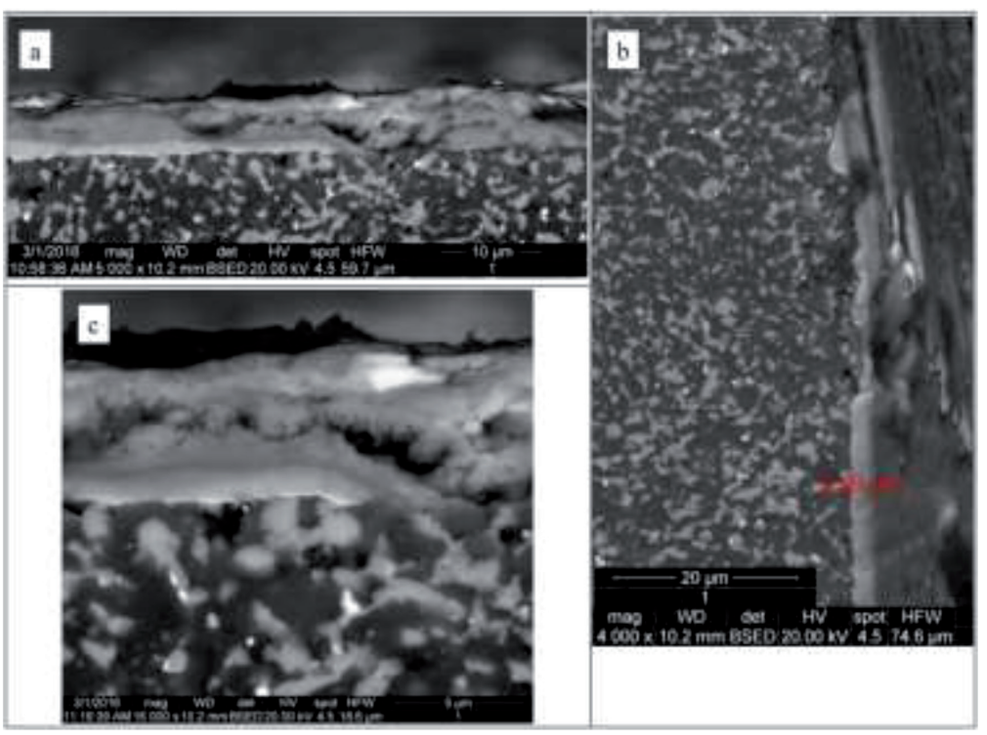

Figure 9.
Wear pattern (a) on the rake face of the Al_2O_3-TiC ceramic insert with the Ti-(Ti,Al)N coating and wear pattern (b) on the flank face of insert with particles of the material being machined after 20 minutes in longitudinal turning of X153CrMoV12 hardened steel at v_c = 250 m/min, f = 0.05 mm/rev, a_p = 0.5 mm [67] (SEM).

4.2 Turning of AISI 52100 (HRC 56–58) hardened steel with tools with (Cr,Al,Si)N-(DLC-Si)-DLC-(DLC-Si), and (Cr,Al,Si)N-DLC coatings

The investigation of the DLC-1 coating structure using TEM reveals the presence of a wear-resistant layer in the amorphous DLC and a (Cr,Al,Si)N transition layer with the columnar structure (**Figure 10a** and **b**) [68]. In its turn, the DLC layer structure includes sublayers of DLC-Si at the border of the (Cr,Al,Si)N layer and the coating surface. The (Cr,Al,Si)N layer is about 0.4 μm thick, and the thickness of the DLC layer is about 1.4 μm.

The DLC-2 coating also has a two-layer structure with a (Cr,Al,Si)N transition layer and a DLC wear-resistant layer (**Figure 10c** and **d**). The thickness of the transition layer is about 0.3 μm, while the thickness of the DLC layer is about 1.1 μm.

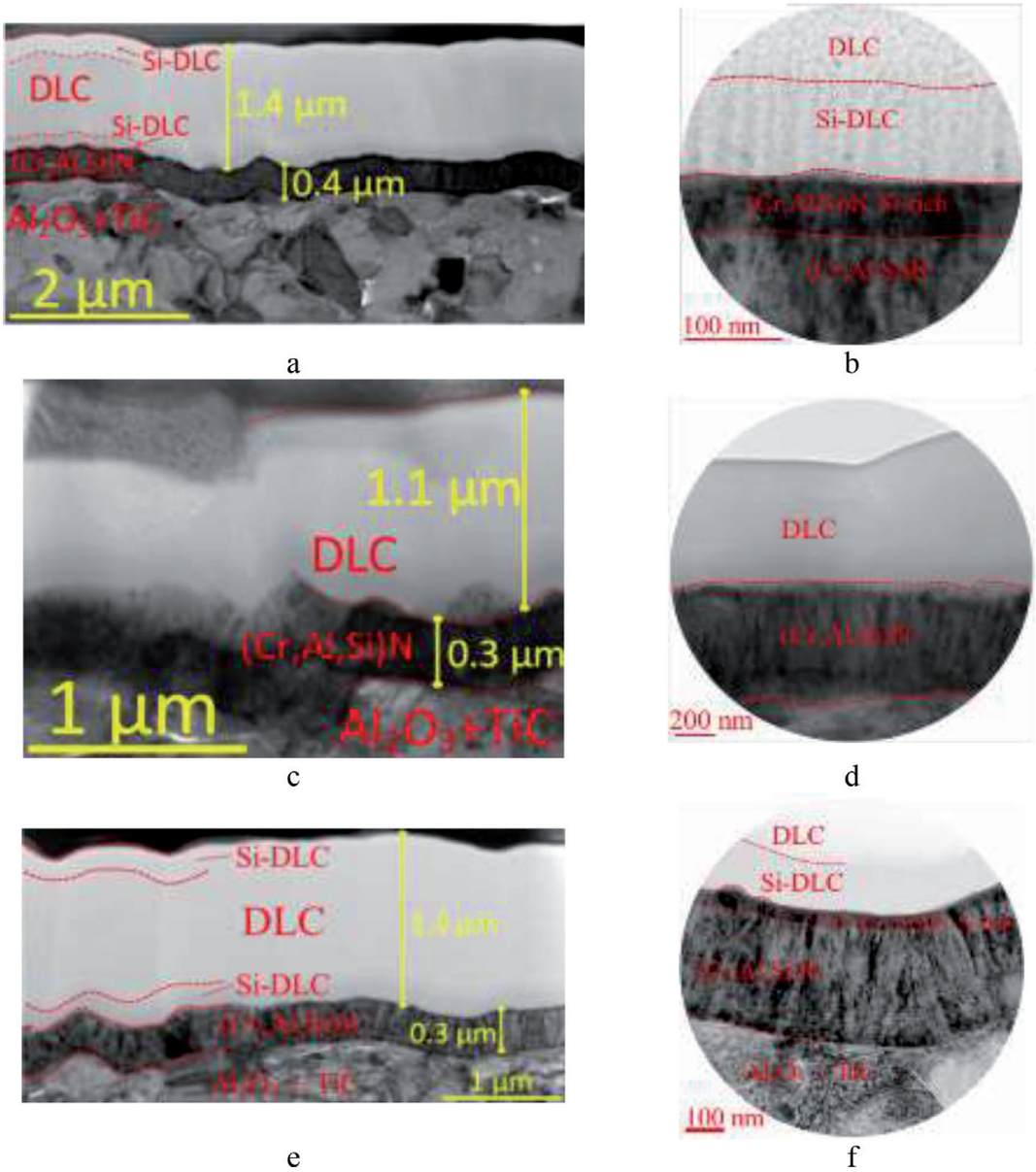

Figure 10.
Internal structure of the coatings under study: (a and b) DLC-1; (c and d) DLC-2; and (e and f) DLC-3 obtained using TEM [68].

The TEM analysis of the cross-section image for the DLC-1 coating (**Figure 10a**) reveals the absence of any clear structure in the DLC layer. The electron diffraction patterns depict a broadened halo, typical for an amorphous structure, while a structure close to columnar can be noticed in the DLC-Si sublayer (**Figure 10b**). The chemical composition of the DLC-Si sublayer includes about 56 at% Si + 43 at% C + 1 at% O. The DLC layer includes about 1 at% Si + 97 at% C + 2 at% O (**Figure 10b**). The (Cr,Al,Si)N layer includes 70 at% Cr + 23at% Al + 7 at% Si. The surface layer of the ceramic substrate Al_2O_3 exhibits signs of diffusion of Cr in the volume of 0.3–0.4 at%. The area around the (Cr,Al,Si)N layer, adjacent to the border of the DLC-Si layer is characterized by an increase content of Si (about 10 at%) to ensure better adhesion with the DLC-Si layer. The high (above 50 at%) content of Si is detected in the transition layer and the surface layer of DLC.

The earlier studies have found that the structure of (Cr,Al,Si)N is characterized by a face-centered NaCl-type lattice with various crystal orientations: (111), (200), and (220) [26, 27]. In the presence of the CrN phase, the phases of Cr, Cr_2N, $CrSi_2$, and Si_3N_4 were also detected [27]. The investigation has also revealed that Si is

present either in the form of a substitutional solid solution in the Cr-Al-N lattice, or in the form of an amorphous Si-N compound that accumulates at the grain boundaries of Cr-Al-N [27, 31, 32]. **Figure 11** exhibits the nanostructure of the (Cr,Al,Si)N layer, characterized by the presence of various phases differing with interplanar spacings and orientations of crystal planes [68].

The formation of a fan-shaped network of microdroplets in the DLC layer, caused by microdroplets of (Cr,Al,Si), embedded in the structure of the DLC layer, is depicted in **Figure 12** [68]. During the process of cutting with a coated tool, active fracture can occur in those areas of the DLC layer. So, during the deposition of the coatings with the structures under study, the minimized number of microdroplets is a key condition to ensure the required working efficiency of the coating.

The (Cr,Al,Si)N layer with its smoothing function plays an essential role during deposition of a DLC-Si layer with regard to the elimination of possible stress concentrators on the surface. In particular, a microdefect which appeared on the surface of the ceramic substrate as a result of conjunction of two grains is depicted in **Figure 13** [68]. When the DLC-Si layer is deposited directly onto a ceramic substrate, such a microdefect can provoke cracking in the DLC-Si structure under the above-described mechanism. The above microdefect is being smoothed by the (Cr,Al,Si)N layer, which forms a smooth surface without serious defects that would be able to act as stress concentration in the DLC layer. With the prime function of the (Cr,Al,Si)

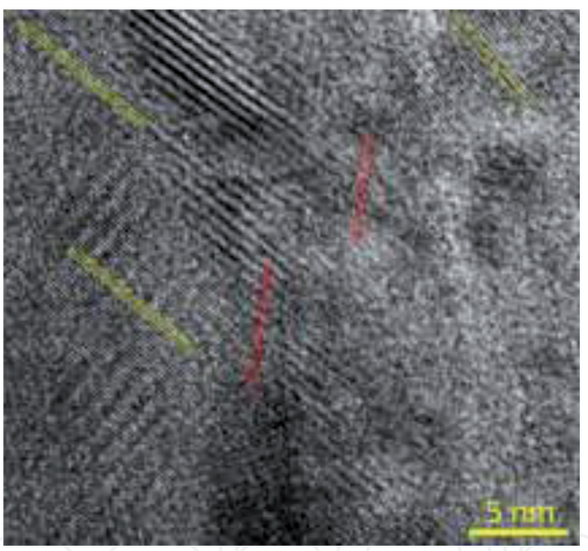

Figure 11.
High-resolution TEM image showing the crystalline structure of the (Cr,Al,Si)N transition layer for DLC-1 [68].

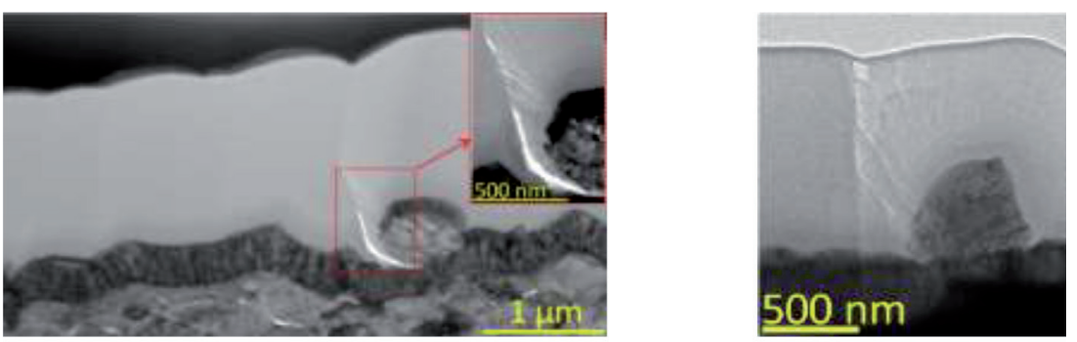

Figure 12.
Influence of embedded microdroplets on forming cracks in the DLC layer for (a) DLC-3 and (b) DLC-2 coatings [68] (TEM).

N layer consisting in the provision of good adhesion between the ceramic substrate and the DLC-Si coating and the formation of a composite structure with a combination of high hardness and brittle fracture resistance, the smoothing functions of the (Cr,Al,Si)N layer are also crucial to secure good coating performance.

Cutting tests are crucial in the assessment of the working efficiency of a coated tool and the performance properties of the very coating. The tests were also conducted to study the dynamics of wear on the rake faces of the uncoated cutting tools made of ceramics and the tools with the DLC-1 and DLC-2 coatings. The tool with the DLC-2 coating proved to have the best resistance to the wear crater formation on the rake face (see **Figure 14**) [68].

The most active formation of a wear crater was detected on the uncoated tool. The active formation of adherents during the cutting is a typical feature of the tool with the DLC-1 coating. This proves high adhesion between the DLC-1 coating and the material being machined. As a result, strong adhesive bond bridges are formed and broken, which leads to a high adhesive-fatigue wear of the tool. At the same time, an abrasive wear with significantly lower adherent formation is typical for the tool with the DLC-2 coating.

The wear pattern on the rake face of the tool was considered in detail (**Figure 10**). The first typical feature was a much more active formation of an adherent of the material being machined for the tool with the DLC-1 coating. At the same time, the uncoated tool and the tool with the DLC-2 coating demonstrated an insignificant formation of such adherents. Based on the obtained results, it can be concluded that there is an

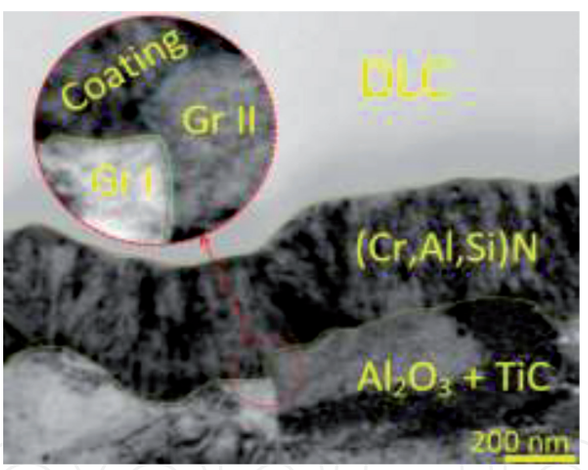

Figure 13.
Example of the smoothing effect of the (Cr,Al,Si)N layer on the DLC-3 coating [68] (TEM).

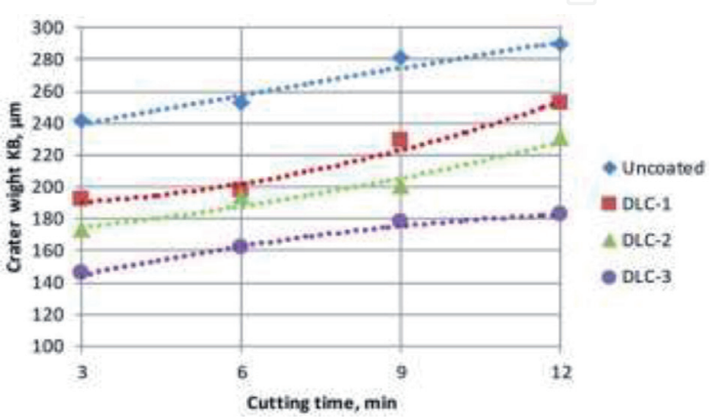

Figure 14.
Dynamics of changes in the crater on the rake face of the tool [68].

increased adhesion between the material of the DLC-1 coating (with a surface sublayer with the high Si content) and the material being machined. The uncoated tool and the tool with the DLC-2 coating are characterized by primarily abrasive wear, accompanied by the formation of typical grooves in the direction of chip flow. The tool with the DLC-1 coating also has similar grooves, but there are also signs of the cutting edge chipping.

Since the flank wear is usually assumed as a limiting factor, its dynamics was considered (**Figure 15**) [68]. The most active flank wear was detected on the tool with the DLC-1 coating. As already stated, this fact can be explained by the high adhesion between the coating and the material being machined. As a result, the tool demonstrated the increased adhesive-fatigue wear. Meanwhile, less active adhesion to the material being machined and lower tendency to chipping were detected on the uncoated tool. At the same time, there is minor chipping in the area of the cutting edge. Finally, the tool with the DLC-2 coating demonstrated a low tendency to the formation of adherents and no visible signs of brittle fracture. Thus, the purely abrasive wear mechanism was typical for the tool with the DLC-2. The tool with the coating DLC-2 exhibited a 17% higher resistance to the flank wear. In combination with its noticeably higher resistance to the formation of a wear crater on the rake face and the more favorable wear pattern (implying the balanced abrasive wear instead of chipping and brittle fracture), the above proves the good prospects of the DLC-2 coating.

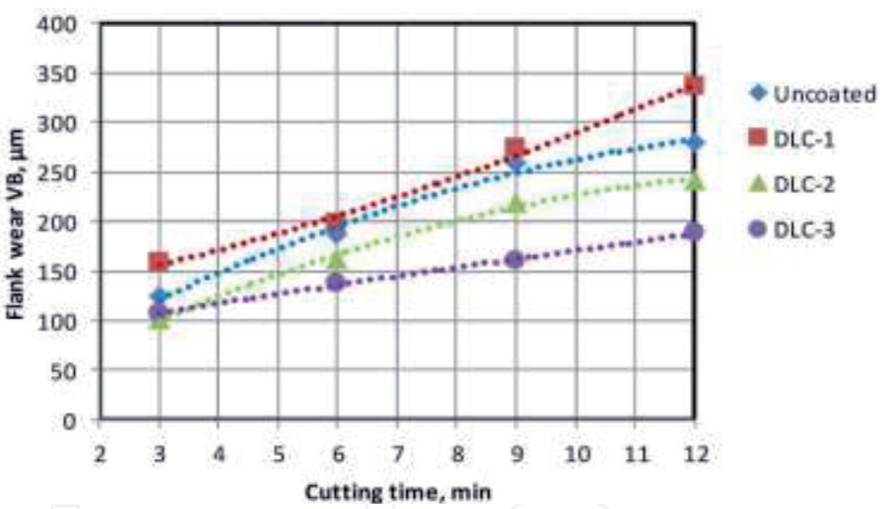

Figure 15.
Tool wear on the flank face depending on the cutting time [68].

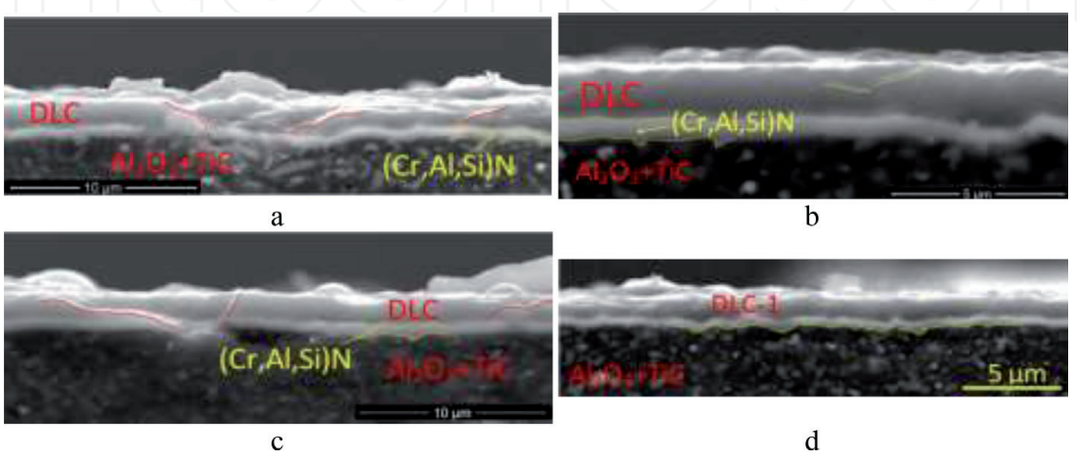

Figure 16.
Investigation of the wear pattern on a cross-section of the tool with the DLC-1 coating [68] (SEM). Through cracks and tears (a, c), minor cracks and intact coating (b, d).

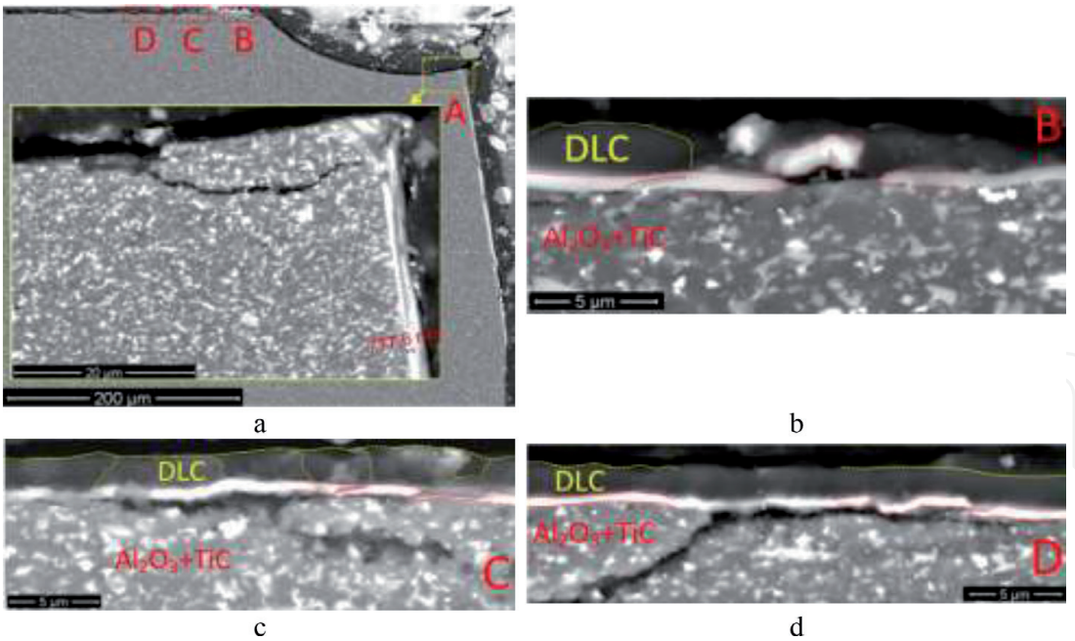

Figure 17.
Investigation of the fracture pattern on a cross-section of the tool with the DLC-2 coating [68] (SEM). General view and a crack passing into a ceramic substrate (a), tearing out of a coating fragment (b), cracks in a coating turning into a substrate (c, d).

For a better understanding of the wear patterns on the samples, cross-sections were made passing through the centre of the wear craters.

Figure 16 demonstrates that the sample with the DLC-1 coating bears clear signs of cutting edge chipping. It is also clear that the coating is retained on the rake face of the tool in the area adjacent to the boundary of the wear crater. On the flank face, in the area adjacent to the flank wear land, the DLC layer failed while the (Cr,Al,Si)N layer was preserved. In general, the coating retains good adhesion to the substrate, and it does not separate from the substrate on the sample with the DLC-1 coating.

The wear process on the DLC-1 coating, especially its upper layer, is characterized by the formation of inclined cracks (**Figure 16a–c**), which in some cases also penetrate into the (Cr,Al,Si)N transition layer (**Figure 16a** and **c**). It is also clear that the surface of the ceramic substrate has a rather complex relief, and the (Cr,Al,Si)N transition layer fills in the microroughness of the surface and thus forms a basis for the DLC layer (**Figure 16d**) [68].

During the consideration of the wear process on the tool with the DLC-2 coating, it can be noticed that the transition layer of this coating demonstrates a higher tendency to brittle fracture compared to the transition layer of the DLC-1 coating (**Figure 17**) [68]. The DLC layer of the DLC-2 coating also bears signs of active brittle fracture. In the area, adjacent to the wear crater (Area B, **Figure 17**), almost complete failure of the DLC layer and partial failure of the transition layer are detected (**Figure 17b**). The brittle fracture of the ceramic substrate, accompanied by microchipping, also takes place. The signs of such brittle fracture are detected throughout the whole contact area on the rake face of the tool.

5. Conclusions

The chapter considered the specific features of the use of wear-resistant coatings deposited to improve the performance properties of ceramic cutting tools. The application of the Ti-(Ti,Al)N-(Zr,Nb,Ti,Al)N multilayer composite coating with a

nanostructured wear-resistant layer and the (Cr,Al,Si)N-(DLC-Si)-DLC-(DLC-Si) and (Cr,Al,Si)N-DLC composite coatings increase the tool life of a ceramic cutting tool by 50–80%.

Following the studies, it has been found that the intensity of the thermal effect on structures of the ceramic substrate may be reduced through the deposition of the developed coatings under study on contact areas of ceramic cutting tools, since such coatings provide better heat removal from the cutting area due to an increased length of the plastic contact.

The use of the DLC-based coatings can both prolong (due to an enhanced resistance to abrasive wear) and shorten (due to higher adhesion) the tool life. It is not advisable to deposit a coating with an increased Si content in the surface layers of the coating, at least for the considered cutting conditions, despite a bit higher hardness of such coating. At the same time, a coating with the high Si content demonstrated a lower tendency to brittle fracture compared to the DLC-2 coating. The use of the (Cr,Al,Si)N transition layer is advisable, since it improves the adhesion between the ceramic substrate and the DLC coating.

The results of the conducted studies prove the prospects for the application of multilayer composite coatings, including those with DLC layers introduced to improve the cutting properties of ceramic cutting tools (both assembled and one-piece tools).

Acknowledgements

This study was supported by a grant of the Russian Science Foundation [Agreement No. 18-19-00312 dated 20 April 2018].

Conflict of interest

The authors declare no conflict of interest.

Author details

Sergey Grigoriev[1], Alexey Vereschaka[2*], Marina Volosova[1], Caterina Sotova[1], Nikolay Sitnikov[3], Filipp Milovich[4] and Nikolay Andreev[4]

1 Moscow State Technological University STANKIN, Moscow, Russia

2 IDTI RAS, Moscow, Russia

3 National Research Nuclear University MEPhI, Moscow, Russia

4 National University of Science and Technology MISiS, Moscow, Russia

*Address all correspondence to: dr.a.veres@yandex.ru

References

[1] Riedel R. Handbook of Ceramic Hard Materials. WILEY-VICH: Weinheim–New York; 2000

[2] López de Lacalle LN, Lamikiz A. Machine Tools for High Performance Machining. Springer, 2009

[3] Sun S, Brandt M, Dargusch MS. Thermally enhanced machining of hard-to-machine materials. A review. International Journal of Machine Tools and Manufacture. 2010;**50**(8):663-680

[4] Rahman M, Wang Z-G, Wong Y-S. A review on high-speed machining of titanium alloys. JSME International Journal, Series C: Mechanical Systems, Machine Elements and Manufacturing. 2006;**49**(1):11-20

[5] Ezugwu EO. High speed machining of aero-engine alloys. Journal of the Brazilian Society of Mechanical Sciences and Engineering. 2004;**26**(1):1-11

[6] Senthil Kumar A, Raja Durai A, Sornakumar T. Machinability of hardened steel using alumina based ceramic cutting tools. International Journal of Refractory Metals and Hard Materials. 2003;**21**(3-4):109-117

[7] Kumar AS, Durai AR, Sornakumar T. Wear behaviour of alumina based ceramic cutting tools on machining steels. Tribology International. 2006;**39**(3):191-197

[8] Grigoriev SN, Vereschaka AA, Vereschaka AS, Kutin AA. Cutting tools made of layered composite ceramics with nano-scale multilayered coatings. Procedia CIRP. 2012;**1**(1):301-306

[9] Vereschaka AS, Grigoriev SN, Sotova ES, Vereschaka AA. Improving the efficiency of the cutting tools made of mixed ceramics by applying modifying nano-scale multilayered coatings. Advanced Materials Research 2013;712-715: 391-394

[10] Vereschaka AS, Grigoriev SN, Tabakov VP, Sotova ES, Vereschaka AA, Kulikov MY. Improving the efficiency of the cutting tool made of ceramic when machining hardened steel by applying nano-dispersed multi-layered coatings. Key Engineering Materials. 2014;**581**:68-73

[11] Vereshchaka AA, Sotova ES, Batako AD, Sedykh MI, Vereshchaka AS. A study of the cutting properties and wear mechanism of ceramic edge tools with nanostructure multilayer composite coatings. Journal of Friction and Wear. 2014;**35**(6):483-488

[12] Vereschaka A, Prilukova J, Vereschaka A, Bublikov J, Aksenenko A. Control of temperature in cutting zone in machining of alloyed casehardened steels by applying a ceramic tool with wear-resistant coatings. Materials Science Forum. 2016;**857**:199-205

[13] Ezugwu EO, Bonney J, Yamane Y. An overview of the machinability of aeroengine alloys. Journal of Materials Processing Technology. 2003;**134**(2):233-253

[14] Kitagawa T, Kubo A, Maekawa K. Temperature and wear of cutting tools in high-speed machining of Inconel 718 and Ti-6Al-6V-2Sn. Wear. 1997;**202**(2):142-148

[15] Devillez A, Schneider F, Dominiak S, Dudzinski D, Larrouquere D. Cutting forces and wear in dry machining of Inconel 718 with coated carbide tools. Wear. 2007;**262**(7-8):931-942

[16] Vereschaka AA, Volosova MA, Krapostin AA, Batako A, Seleznev AE. Increased operating properties of

cutting ceramics by application of nanostructured multilayer wear-resistant coating. Journal of Nano Research. 2017;**50**:90-104

[17] Merchant ME. Mechanics of the metal cutting process. II. Plasticity conditions in orthogonal cutting. Journal of Applied Physics. 1945;**16**(6):318-324

[18] Tounsi N, Vincenti J, Otho A, Elbestawi MA. From the basic mechanics of orthogonal metal cutting toward the identification of the constitutive equation. International Journal of Machine Tools and Manufacture. 2002;**42**(12):1373-1383

[19] Volosova MA, Grigor'ev SN, Kuzin VV. Effect of Titanium Nitride Coating on Stress Structural Inhomogeneity in Oxide-Carbide Ceramic. Part 4.Action of Heat Flow. Refract Ind Ceram 2015;56:91-96

[20] Kuzin VV, Grigor'ev SN, Volosova MA. Effect of a TiC coating on the stress-strain state of a plate of a high-density nitride ceramic under nonsteady thermoelastic conditions. Refractories and Industrial Ceramics. 2014;**54**:376-380

[21] Czechowski K, Pofelska-Filip I, Królicka B, Szlosek P, Smuk B, Wszołek J, et al. Effect of nitride nano-scale multilayer coatings on functional properties of composite ceramic cutting inserts. Bulletin of the Polish Academy of Sciences Technical Sciences. 2005;**53**(4):425-431

[22] Sokovic M, Kopac J, Dobrzanski LA, Mikula J, Golombek K, Pakula D. Cutting characteristics of PVD and CVD - coated ceramic tool inserts. Tribology in Industry. 2006;**28**:3-8

[23] Aslantas K, Ucun I, Cicek A. Tool life and wear mechanism of coated and uncoated Al2O3/TiCN mixed ceramic tools in turning hardened alloy steel. Wear. 2012;**274-275**:442-451

[24] Qin J, Long Y, Zeng J, Wu S. Continuous and varied depth-of-cut turning of gray cast iron by using uncoated and TiN/Al2O3 coated silicon nitride-based ceramic tools. Ceramics International. 2014;**40**(8):12245-12251

[25] Long Y, Zeng J, Yu D, Wu S. Cutting performance and wear mechanism of Ti-Al-N/Al-Cr-O coated silicon nitride ceramic cutting inserts. Ceramics International. 2014;**40**(7):9889-9894

[26] Long Y, Zeng J, Yu D, Wu S. Microstructure of TiAlN and CrAlN coatings and cutting performance of coated silicon nitride inserts in cast iron turning. Ceramics International. 2014;**40**(7):9889-9894

[27] Mali NM, Mahender T. Wear analysis of single point cutting tool with and without coating. IJREAT International Journal of Research in Engineering & Advanced Technology. 2015;**3**(3):49-57

[28] Enke K. Upgrading of technical ceramics by DLC-layers. Keramische Zeitschrift. 1998;**50**(12):1022-1025

[29] Enke K. Dry machining and increase of endurance of machine parts with improved doped DLC coatings on steel, ceramics and aluminium. Surface and Coatings Technology. 1999;**116-119**:488-491

[30] Fukuhara T, Kato M, Nishimura S, Ikegami N. Application of ceramics to seal materials. Toraibarojisuto/Journal of Japanese Society of Tribologists. 2018;**63**(12):824-829

[31] Gomes JR, Camargo SS Jr, Simao RA, Carrapichano JM, Achete CA, Silva RF. Tribological properties of silicon nitride ceramics coated with DLC and DLC-Si

against 316L stainless steel. Vacuum. 2007;**81**:1448-1452

[32] Vila M, Carrapichano JM, Gomesc JR, Camargo SS Jr, Achete CA, Silva RF. Ultra-high performance of DLC-coated Si3N4 rings for mechanical seals. Wear. 2008;**265**:940-944

[33] Nie C, Zheng D, Gu L, Zhao X, Wang L. Comparison of interface mechanics characteristics of DLC coatingdeposited on bearing steel and ceramics. Applied Surface Science. 2014;**317**:188-197

[34] Zhang C, Gu L, Zheng D. Tribological Property Analyses of DLC Films on Ceramic Ball Surfaces With 3-D FEA Method and Experiments. ASME/STLE 2012 International Joint Tribology Conference Denver, Colorado, USA, October 7-10, 2012

[35] Gu L, Tang G, Zhang C, Jing C, Wang L. Self-Lubricated Modification for Silicon Nitride Ceramic Ball Surface. STLE/ASME 2010 International Joint Tribology Conference, 2010 Paper No. IJTC2010-41161, 59-60

[36] Wua D, Ren S, Pu J, Lu Z, Zhang G, Wang L. A comparative study of tribological characteristics of hydrogenated DLC film sliding against ceramic mating materials for helium applications. Applied Surface Science. 2018;**441**:884-894

[37] Jian-guang, Zhai Yi-qi, Wang Tae-gyu, Kim Jung-il Song. Finite element and experimental analysis of Vickers indentation testing on Al_2O_3 with diamond-like carbon coating. Journal of Central South University, 2012;19(5):1175-1181

[38] Hamdy AS. Electrochemical behavior of diamond-like-carbon coatings deposited on AlTiC (Al_2O_3 + TiC) ceramic composite substrate in HCl solution. Electrochimica Acta. 2011;**56**:1554-1562

[39] Bisht A, Chockalingam S, Tripathi RK, Dwivedi N, Dayal S, Kumar S, et al. Improved surface properties of β-SiAlON by diamond-like carbon coatings. Diamond & Related Materials. 2013;**36**:44-50

[40] Cho DH, Lee YZ. Evaluation of ring surfaces with several coatings for friction, wear and scuffing life. Transactions of Nonferrous Metals Society of China (English Edition). 2009;**19**(4):992-996

[41] Kato K. Tribology of advanced ceramics and hard coatings. Key Engineering Materials 2004;264-268(I):449-452

[42] Kato K. Tribology of ceramics and hard coatings. Materialwissenschaft und Werkstofftechnik. 2003;**34**(10-11):1003-1007

[43] Vereshchaka AA, Vereshchaka AS, Mgaloblishvili O, Morgan MN, Batako AD. Nano-scale multilayered-composite coatings for the cutting tools. Int. J. Adv. Manuf. Tech. 2014;**72**(1-4):303-317

[44] Vereschaka A, Tabakov V, Grigoriev S, Sitnikov N, Oganyan G, Andreev N, et al. Investigation of wear dynamics for cutting tools with multilayer composite nanostructured coatings in turning constructional steel. Wear. 2019;**420-421**:17-37. DOI: 10.1016/j.wear.2018.12.033

[45] Vereschaka A, Tabakov V, Grigoriev S, Aksenenko A, Sitnikov N, Oganyan G, et al. Effect of adhesion and the wear-resistant layer thickness ratio on mechanical and performance properties of ZrN - (Zr,Al,Si) N coatings. Surface and Coating Technology. 2019;**357**:218-234

[46] Vereschaka AA, Grigoriev SN, Sitnikov NN, Batako AD. Delamination and longitudinal cracking in multi-layered composite nano-structured

coatings and their influence on cutting tool life. Wear 2017;390-391:209-219

[47] Vereschaka A, Tabakov V, Grigoriev S, Sitnikov N, Andreev N, Milovich F. Investigation of wear and diffusion processes on rake faces of carbide inserts with Ti-TiN-(Ti,Al,Si) N composite nanostructured coating. Wear 2018;416-417:72-80

[48] Vereschaka A, Tabakov V, Grigoriev S, Sitnikov N, Milovich F, Andreev N, et al. Investigation of the influence of the thickness of nanolayers in wear-resistant layers of Ti-TiN-(Ti,Cr,Al)N coating on destruction in the cutting and wear of carbide cutting tools. Surface and Coating Technology. 2020;**385**:125402

[49] Vereschaka A, Aksenenko A, Sitnikov N, Migranov M, Shevchenko S, Sotova C, et al. Effect of adhesion and tribological properties of modified composite nano-structured multi-layer nitride coatings on WC-Co tools life. Tribology International. 2018;**128**:313-327

[50] Grigoriev S, Vereschaka A, Milovich F, Tabakov V, Sitnikov N, Andreev N, et al. Investigation of multicomponent nanolayer coatings based on nitrides of Cr, Mo, Zr, Nb, and Al. Surface and Coatings Technology. 2020;**401**:126258

[51] Lubwama M, Corcoran B, Sayers K, Kirabira JB, Sebbit A, McDonnell KA, et al. Adhesion and composite micro-hardness of DLC and Si-DLC films deposited on nitrile rubber. Surface and Coating Technology. 2012;**206**:4881-4886

[52] Qiang L, Bai C, Gong Z, Liang A, Zhang J. Microstructure, adhesion and tribologicalbehaviors of Si interlayer/ Si T doping diamond-like carbon film developed on nitrile butadiene rubber. Diamond and Related Materials. 2019;**92**:208-218

[53] Hofmann D, Kunkel S, Bewilogua K, Wittorf R. From DLC to Si-DLC based layer systems with optimized properties for tribological applications. Surface and Coating Technology. 2013;**215**:357-363

[54] Park I-W, Kang DS, Moore JJ, Kwon SC, Rha JJ, Kim KH. Microstructures, mechanical properties, and tribological behaviors of Cr–Al–N, Cr–Si–N, and Cr–Al–Si–N coatings by a hybrid coating system. Surface and Coating Technology. 2007;**201**:5223-5227

[55] Miyake T, Kishimoto A, Hasegawa H, Tribological properties and oxidation resistance of (Cr,Al,Y) N and (Cr,Al,Si)N films synthesized by radio-frequency magnetron sputtering method, Surface and Coating Technology 2010;205:290-294.

[56] Ding J, Zhang T, Yun JM, Kang MC, Wang Q, Kim KH. Microstructure, mechanical, oxidation and corrosion properties of the Cr-Al-Si-N coatings deposited by a hybrid sputtering system. Coat. 2017;**7**:119

[57] Vereschaka A, Tabakov V, Grigoriev S, Sitnikov N, Oganyan G, Andreev N, et al. Investigation of wear dynamics for cutting tools with multilayer composite nanostructured coatings in turning constructional steel. Wear. 2019;**420-421**:17-37

[58] Vereschaka A, Aksenenko A, Sitnikov N, Migranov M, Shevchenko S, Sotova C, et al. Effect of adhesion and tribological properties of modified composite nano-structured multi-layer nitride coatings on WC-Co tools life. Tribology International. 2018;**128**:313-327

[59] Vereschaka AA, Grigoriev SN, Sitnikov NN, Batako A. Delamination and longitudinal cracking in multi-layered composite nano-structured coatings and their influence on cutting tool life. Wear. 2017;**390-391**:209-219

[60] Kuzin VV, Grigoriev SN, Fedorov MY. Role of the thermal factor in the wear mechanism of ceramic tools. Part 2: Microlevel. Journal of Friction and Wear. 2015;**36**(1):40-44

[61] Metel A, Bolbukov V, Volosova M, Grigoriev S, Melnik Y. Equipment for deposition of thin metallic films bombarded by fast argon atoms. Instruments and Experimental Techniques. 2014;**57**(3):345-351

[62] Metel AS, Grigoriev SN, Melnik YA, Bolbukov VP. Characteristics of a fast neutral atom source with electrons injected into the source through its emissive grid from the vacuum chamber. Instruments and Experimental Techniques. 2012;**55**(2):288-293

[63] Metel A, Bolbukov V, Volosova M, Grigoriev S, Melnik Y. Source of metal atoms and fast gas molecules for coating deposition on complex shaped dielectric products. Surface and Coating Technology. 2013;**225**:34-39

[64] Grigoriev SN, Sobol OV, Beresnev VM, Serdyuk IV, Pogrebnyak AD, Kolesnikov DA, et al. Tribological characteristics of (TiZrHfVNbTa)N coatings applied using the vacuum arc deposition method. Journal of Friction and Wear. 2014;**35**(5):359-364

[65] Vereschaka AA, Grigoriev SN, Vereschaka AS, Popov AY, Batako AD. Nano-scale multilayered composite coatings for cutting tools operating under heavy cutting conditions. Procedia CIRP. 2014;**14**:239-244

[66] Vereschaka AA, Volosova MA, Grigoriev SN, Vereschaka AS. Development of wear-resistant complex for high-speed steel tool when using process of combined cathodic vacuum arc deposition. Procedia CIRP. 2013;**9**:8-12

[67] Vereschaka AA, Volosova MA, Batako A, Vereschaka AS, Sitnikov NN, Seleznev AE. Nano-scale multi-layered coatings for improved efficiency of ceramic cutting tools. International Journal of Advanced Manufacturing Technology. 2017;**90**:27-43

[68] Grigoriev SN, Volosova MA, Vereschaka AA, Sitnikov NN, Milovich F, Bublikov JI, et al. Properties of (Cr,Al,Si)N-(DLC-Si) composite coatings deposited on a cutting ceramic substrate. Ceramics International. 2020;**46**(11):18241-18255